Journal of Magnetic Resonance 196 (2009) 84–87

Contents lists available at ScienceDirect

Journal of Magnetic Resonance

journal homepage: www.elsevier.com/locate/jmr

Communication

# Measurement of sample temperatures under magic-angle spinning from the chemical shift and spin-lattice relaxation rate of $^{79}$Br in KBr powder

Kent R. Thurber, Robert Tycko *

*Laboratory of Chemical Physics, National Institute of Diabetes and Digestive and Kidney Diseases, National Institutes of Health, Building 5, Room 112, Bethesda, MD 20892-0520, USA*

ARTICLE INFO

*Article history:*
Received 1 August 2008
Revised 22 September 2008
Available online 25 September 2008

*Keywords:*
Solid state NMR
Magnetic resonance
Magic-angle spinning
Temperature calibration

ABSTRACT

Accurate determination of sample temperatures in solid state nuclear magnetic resonance (NMR) with magic-angle spinning (MAS) can be problematic, particularly because frictional heating and heating by radio-frequency irradiation can make the internal sample temperature significantly different from the temperature outside the MAS rotor. This paper demonstrates the use of $^{79}$Br chemical shifts and spin-lattice relaxation rates in KBr powder as temperature-dependent parameters for the determination of internal sample temperatures. Advantages of this method include high signal-to-noise, proximity of the $^{79}$Br NMR frequency to that of $^{13}$C, applicability from 20 K to 320 K or higher, and simultaneity with adjustment of the MAS axis direction. We show that spin-lattice relaxation in KBr is driven by a quadrupolar mechanism. We demonstrate a simple approach to including KBr powder in hydrated samples, such as biological membrane samples, hydrated amyloid fibrils, and hydrated microcrystalline proteins, that allows direct assessment of the effects of frictional and radio-frequency heating under experimentally relevant conditions.

Published by Elsevier Inc.

## 1. Introduction

In nuclear magnetic resonance (NMR) with magic-angle spinning (MAS), the sample is generally at the center of a rapidly spinning rotor, preventing placement of a conventional temperature sensor at the sample position. The sample temperature can be strongly affected by frictional heating of the rotor (particularly at high MAS frequencies) or absorption of energy from radio-frequency (rf) electric fields (particularly in hydrated samples or other lossy samples). Additionally, when separate gas sources are used for MAS drive and bearings and for temperature control, the temperature of the gas that surrounds the MAS rotor may be uncertain. Temperature gradients across the MAS rotor and in the surrounding gas create further complications.

Several techniques for determination of internal sample temperatures have been proposed, including calibrations by known phase transition temperatures [1–5] and measurements of temperature-dependent chemical shifts for $^{13}$C in samarium acetate [6], $^{15}$N in TTAA [7], $^{1}$H in bulk water [8], $^{1}$H in methanol soaked into TTMSS [9], $^{207}$Pb in lead nitrate [10–14], $^{119}$Sn in $Sm_2Sn_2O_7$ and other compounds [15,16], $^{31}$P in $(VO)_2P_2O_7$ [17], and $^{1}$H and $^{31}$P in aqueous solutions of TmDOTP [18]. Alternatively, the temperature dependence of a spin-lattice relaxation rate ($1/T_1$) can be used, *e.g.*, that of $^{7}$Li [19]. The shift of quartz crystal resonances [20] and the $^{35}$Cl NQR frequency of $NaClO_3$ [21,22] have also been proposed as useful temperature-dependent parameters.

In this Communication, we describe temperature measurements based on the chemical shift and $T_1$ of $^{79}$Br in KBr powder. This method has a number of advantages, especially for $^{13}$C MAS NMR: (i) The $^{79}$Br NMR frequency differs from the $^{13}$C NMR frequency by only 0.4%, allowing the $^{13}$C channel of the NMR probe to be used with only minor retuning; (ii) The temperature range from 20 to 320 K or higher can be covered; (iii) The $^{79}$Br signal can be used for both temperature and magic-angle monitoring [23]; (iv) The $^{79}$Br signal is strong and $T_1$ is short at temperatures above 40 K. Small quantities of KBr are therefore sufficient, which can be included in the sample without sacrificing much sample volume as described below. Additionally, KBr is not highly toxic.

## 2. Temperature-dependent spin-lattice relaxation

Fig. 1a shows the temperature dependence of $T_1$ for $^{79}$Br in KBr. $T_1$ changes by almost three orders of magnitude from 100 to 15 K, providing very good temperature sensitivity. Although the temperature dependence is weaker at higher temperatures, the fast spin-lattice relaxation ($T_1 = 75 \pm 3$ ms at 296 K) allows rapid measurement with high signal-to-noise, so that $T_1$ measurements can be used to determine sample temperatures up to at least 320 K.

Fig. 1b compares $T_1$ values for $^{79}$Br and $^{81}$Br. Both are spin-3/2 isotopes with high abundance and similar gyromagnetic ratios, allowing comparative measurements without modification of the

* Corresponding author. Fax: +1 301 496 0825.
*E-mail address:* robertty@mail.nih.gov (R. Tycko).

1090-7807/$ - see front matter Published by Elsevier Inc.
doi:10.1016/j.jmr.2008.09.019

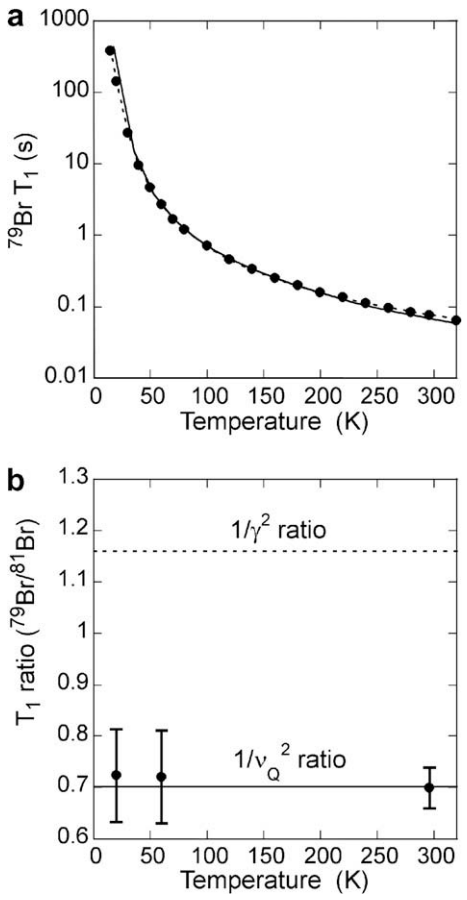


**Fig. 1.** (a) $^{79}$Br spin-lattice relaxation time $T_1$ in KBr powder (static sample) as a function of temperature. The solid line is a theoretical expression for quadrupolar relaxation due to phonons [27,28], with the overall normalization fit to the experimental result at 70 K. The dashed line is the empirical expression given in the text. (b) Ratio of $T_1$ values for $^{79}$Br and $^{81}$Br in KBr as a function of temperature. Solid and dashed lines show the expected ratios for quadrupolar and magnetic relaxation, respectively. $T_1$ values were measured at 9.4 T.

NMR probe. For quadrupolar relaxation, $1/T_1$ is proportional to the quadrupole interaction squared, *i.e.*, $1/T_1 \propto \nu_Q{}^2$; for magnetic relaxation, $1/T_1$ is proportional to the magnetic interaction squared, *i.e.*, $1/T_1 \propto \gamma^2$ [24]. Thus, the ratio of the $^{81}$Br relaxation rate to the $^{79}$Br relaxation rate is predicted to be 0.701 for quadrupolar relaxation and 1.16 for magnetic relaxation [25]. Data in Fig. 1b demonstrate that spin-lattice relaxation in KBr is dominated by quadrupolar interactions down to at least 20 K. This result suggests that paramagnetic impurities, which might vary between samples, do not play a significant role. In fact, our $T_1$ measurements on KBr powder ground with a mortar and pestle are consistent with previous measurements on an optically pure single crystal [26].

The experimental $T_1$ data for $^{79}$Br fit the following empirical expression (dashed line in Fig. 1a) to within 5% between 20 K and 296 K: $T_1 = 0.0145 + 5330T^{-2} + (1.42 \times 10^7)T^{-4} + (2.48 \times 10^9)T^{-6}$ (seconds). This empirical expression is similar to the theoretical temperature dependence for quadrupolar relaxation using a Debye distribution for lattice phonons. The solid line in Fig. 1a shows the theoretical expression with only one adjustable parameter, the overall normalization of the relaxation rate [27,28]. Well above the Debye temperature of $\Theta_D$ = 177 K [26,29], $T_1$ is proportional to $T^{-2}$ in theory, consistent with the experimental results. Below the Debye temperature, phonons are frozen out, and the temperature dependence is stronger. In the low-temperature limit, $T_1$ is proportional to $T^{-7}$ in theory [28]. However, this limit is only a good approximation at temperatures below our measurement range ($T < 0.02\ \Theta_D$ = 3.5 K) [28].

$T_1$ data in Fig. 1 were measured at 9.4 T in a non-spinning helium-cooled probe, based on a customized Janis SuperTran continuous flow cryostat, that provides accurate sample temperatures [30–32] using both Cernox and platinum resistor temperature sensors (Lake Shore Cryotronics). The $T_1$ values were measured by saturation-recovery of the central NMR line (saturation with 5–80 $\pi/2$ pulses with 0.3–10 ms gaps), using a single-exponential fit. In general, spin-lattice relaxation of a nucleus with spin > 1/2 is not single-exponential, and the relaxation of the central and satellite transitions will be different [33]. However, for KBr under MAS, we have found the $T_1$ values of the central NMR line and the MAS sidebands to be equal, both at room temperature and 25 K. We attribute this observation to fast spin exchange among the different transitions across the fairly narrow width (~25 kHz) of the quadrupolar-broadened lineshape. The spin–spin relaxation time of $^{81}$Br is 400 μs at room temperature [34], and we have measured ~200 μs for $^{79}$Br at 30 K (non-spinning). Also, $T_1$ for $^{79}$Br at different MAS frequencies $\nu_{MAS}$ does not show any change other than that expected from frictional heating up to at least $\nu_{MAS}$ = 16 kHz (see Fig. 2).

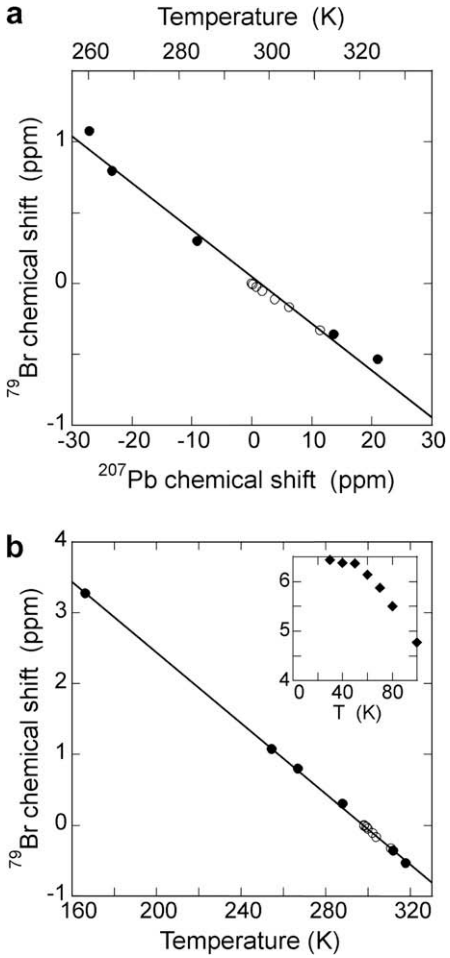


**Fig. 2.** (a) Correlation of the $^{79}$Br chemical shift of KBr powder under MAS with that of $^{207}$Pb in lead nitrate, using identical conditions for the two measurements. The temperature scale is determined from the reported temperature dependence of the $^{207}$Pb chemical shift [10]. (b) Temperature dependence of the $^{79}$Br chemical shift of KBr powder under MAS, with the temperature scale determined by $^{79}$Br $T_1$ measurements. Inset shows the $^{79}$Br chemical shift in a static sample at lower temperatures. Solid circles in (a) and (b) are data in which heated or cooled nitrogen gas was used to vary the sample temperature. Open circles are data in which the sample temperature was raised above room temperature by MAS at various spinning frequencies. Solid lines are linear fits. Chemical shifts are normalized to 0.0 ppm at 296 K (100.025761 MHz for $^{79}$Br, 83.227189 MHz for $^{207}$Pb).

### 3. Temperature-dependent chemical shifts

Sample temperatures can also be determined from the temperature dependence of the $^{79}$Br chemical shift. This can be a more rapid and convenient approach than $T_1$ measurements. Fig. 2a compares the $^{79}$Br chemical shift in KBr powder to the $^{207}$Pb chemical shift in lead nitrate at various temperatures, measured with a Varian 3.2 mm MAS probe at 9.4 T. As previously shown by Bielecki and Burum [10], the $^{207}$Pb shift has a 0.753 ppm/K temperature dependence, which is used to calibrate the temperature axis in Fig. 2a. Both chemical shifts are set to 0.0 ppm at 296 K. Sample temperatures in Fig. 2a were varied from 260 to 324 K by supplying heated or cooled nitrogen gas to the probe's variable-temperature (VT) input (filled circles) or by varying $\nu_{MAS}$ (open circles). Corresponding KBr and lead nitrate measurements were made under identical conditions of $\nu_{MAS}$, VT gas flow, and VT gas temperature. A linear fit of the $^{79}$Br data yields a $-0.0249 \pm 0.0015$ ppm/K slope.

Fig. 2b shows temperature-dependent $^{79}$Br chemical shift measurements in which sample temperatures were determined from the $^{79}$Br $T_1$ measurements described above. A linear fit of these data yields a $-0.0250 \pm 0.0004$ ppm/K slope, in excellent agreement with the slope determined from Fig. 2a. The linear dependence on temperature breaks down below 100 K, as shown by data in the inset to Fig. 2b, which were obtained in the non-spinning cryostat.

To use KBr as a temperature sensor within another sample of interest (especially a hydrated sample where dissolution of KBr powder would occur), we use the simple MAS rotor configuration depicted in Fig. 3. A plug of KBr powder (2.0 mg) is loaded into a hole in the end of a modified nylon screw (2–56 gauge), which is then threaded into one of the rotor end caps. Epoxy or cyanoacrylate glue is used to seal the KBr powder in place. Equivalent configurations are readily devised, depending on the rotor diameter or other factors. Fig. 3 shows examples of $^{79}$Br spectra recorded at 14.1 T with a Varian 5 mm MAS probe when the rotor is filled with a hydrated multilamellar 1,2,-dioleoyl-sn-glycero-3-phosphocholine(DOPC) lipid bilayer sample. In Fig. 3a, the spectra were recorded at various $\nu_{MAS}$ values and with various VT nitrogen gas temperatures (100 scfh flow rate), using single-pulse excitation of $^{79}$Br and no irradiation on the proton channel of the probe. Each spectrum was acquired in about 2 sec (16 scans, 0.1 s recycle delay). Central-transition $^{79}$Br NMR frequencies were determined to ±2 Hz by fitting the NMR lines to Gaussian/Lorentzian functions, corresponding to ±0.5 °C uncertainties in actual sample temperatures. Dependences of the sample temperature on $\nu_{MAS}$ and VT gas temperature are easily measured.

In Fig. 3b, the spectra were recorded at $\nu_{MAS} = 7.00$ kHz with various recycle delays and with a 71 kHz proton decoupling field during the 30.72 ms $^{79}$Br free induction decay. Dependences on the duty factor (*i.e.*, average decoupling power) are easily measured and are quite large for recycle delays in the 1–2 s range, as commonly used in solid state $^{13}$C and $^{15}$N NMR experiments. Results in Fig. 3 demonstrate the simplicity of internal sample temperature measurements based on $^{79}$Br NMR, as well as the importance of doing such measurements prior to MAS NMR experiments on temperature-sensitive samples. To mimic experiments that involve multiple time periods with different decoupling levels, appropriate blocks of rf irradiation can be applied to the proton channel before excitation of the $^{79}$Br free induction decay.

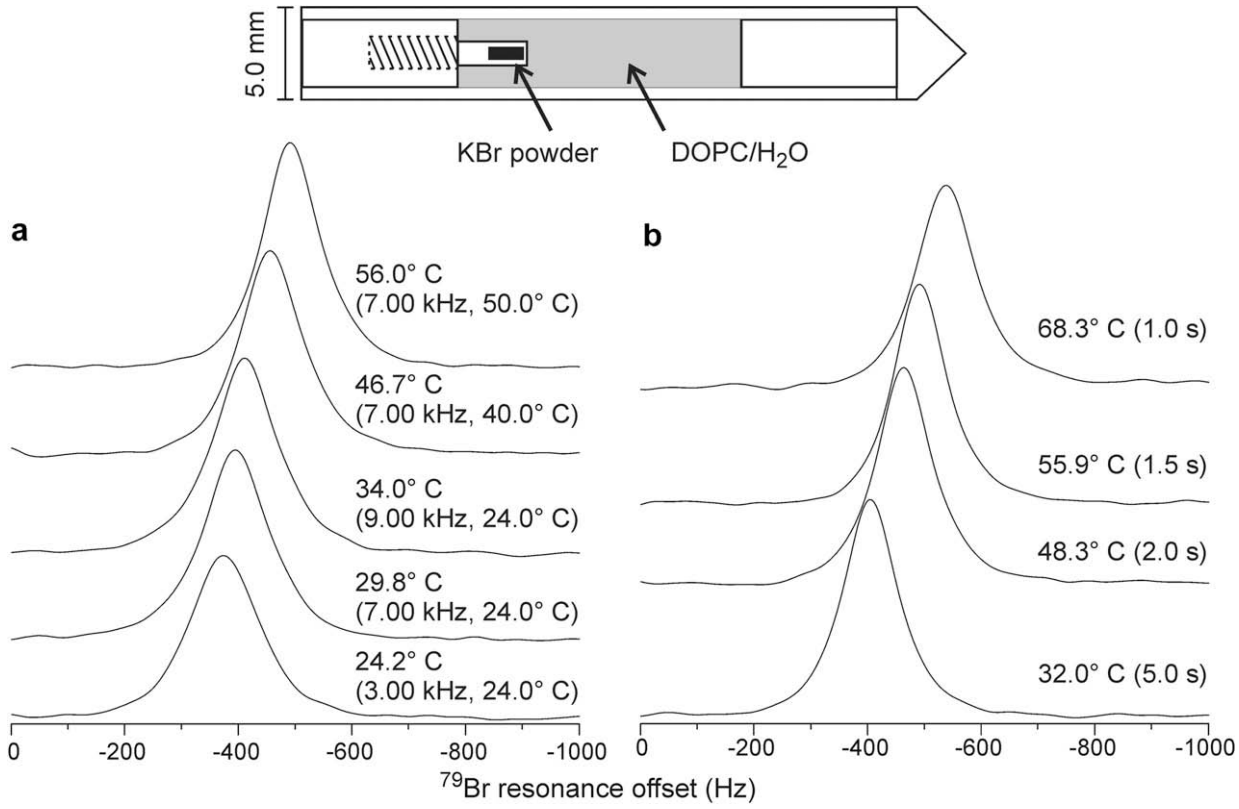


**Fig. 3.** (a) $^{79}$Br NMR spectra of KBr powder within a hydrated DOPC sample, obtained without proton decoupling at MAS frequencies and nominal temperatures indicated in parentheses. Actual sample temperatures reported above the parentheses were determined from the $^{79}$Br NMR frequencies. Spectra were obtained at 14.1 T with 16 scans, and show only the central transition. Nominal temperatures are the temperature of nitrogen gas used for temperature control. The NMR frequency corresponding to room temperature (22.0 °C) was determined at 2.00 kHz MAS, where frictional heating is negligible. (b) Effect of proton decoupling (71 kHz rf field strength, 30.72 ms free induction decay length) on sample temperature. Spectra were acquired in 32 scans with the indicated recycle delays after equilibration by repeated pulsing for at least 1 min.

## 4. Conclusion

We expect $^{79}$Br chemical shift and $T_1$ measurements to be useful for sample temperature determinations in a variety of settings, including MAS NMR studies of the structural properties of biomolecular systems and studies of molecular dynamics, thermodynamics, or chemical kinetics based on temperature-dependent spin relaxation rates, lineshapes, or NMR signal amplitudes. In addition, progress on the development of technology for low-temperature MAS NMR [22,35] and dynamic nuclear polarization [36] requires measurements of internal sample temperatures and will be facilitated by the methods described above.

## Acknowledgments

This work was supported by the Intramural Research Program of the National Institute of Diabetes and Digestive and Kidney Diseases (NIDDK), a component of the National Institutes of Health (NIH), and by a grant from the NIH Intramural AIDS Targeted Antiviral Program. We thank Dr. Junxia Lu for assistance with the measurements in Fig. 3.

## References

[1] H.H. Limbach, J. Hennig, R. Kendrick, C.S. Yannoni, Proton-transfer kinetics in solids: tautomerism in free base porphines by $^{15}$N CPMAS NMR, J. Am. Chem. Soc. 106 (1984) 4059–4060.
[2] J.F. Haw, R.A. Crook, R.C. Crosby, Solid–solid phase transitions for temperature calibration in magic-angle spinning, J. Magn. Reson. 66 (1986) 551–554.
[3] T. Bjorholm, H.J. Jakobsen, $^{31}$P MAS NMR of $P_4S_3$. Crystalline-to-plastic phase transition induced by MAS in a double air-bearing stator, J. Magn. Reson. 84 (1989) 204–211.
[4] K.L. Anderson-Altmann, D.M. Grant, A solid-state $^{15}$N NMR study of the phase transitions in ammonium nitrate, J. Phys. Chem. 97 (1993) 11096–11102.
[5] A.N. Klymachyov, N.S. Dalal, Squaric acid as an internal standard for temperature measurements in $^{13}$C MAS NMR, Solid State Nucl, Magn. Reson. 7 (1996) 127–134.
[6] G.C. Campbell, R.C. Crosby, J.F. Haw, $^{13}$C chemical shifts which obey the Curie law in CP/MAS NMR spectra. The first CP/MAS chemical-shift thermometer, J. Magn. Reson. 69 (1986) 191–195.
[7] B. Wehrle, F. Aguilar-Parrilla, H.-H. Limbach, A novel $^{15}$N chemical shift NMR thermometer for magic-angle spinning experiments, J. Magn. Reson. 87 (1990) 584–591.
[8] S.V. Dvinskikh, V. Castro, D. Sandstrom, Heating caused by radio-frequency irradiation and sample rotation in $^{13}$C magic-angle spinning NMR studies of lipid membranes, Magn. Reson. Chem. 42 (2004) 875–881.
[9] A.E. Aliev, K.D.M. Harris, Simple technique for temperature calibration of a MAS probe for solid state NMR spectroscopy, Magn. Reson. Chem. 32 (1994) 366–369.
[10] A. Bielecki, D.P. Burum, Temperature dependence of $^{207}$Pb MAS spectra of solid lead nitrate. An accurate, sensitive thermometer for variable temperature MAS, J. Magn. Reson. A 116 (1995) 215–220.
[11] L.C.M.v. Gorkom, J.M. Hook, M.B. Logan, J.V. Hanna, R.E. Wasylishen, Solid state lead-207 NMR of lead(II) nitrate: localized heating effects at high magic-angle spinning speeds, Magn. Reson. Chem. 33 (1995) 791–795.
[12] P.K. Isbester, A. Zalusky, D.H. Lewis, M.C. Douskey, M.J. Pomije, K.R. Mann, E.J. Munson, NMR probe for heterogeneous catalysis with isolated reagent flow and magic-angle spinning, Catal. Today 49 (1999) 363–375.
[13] T. Takahashi, H. Kawashima, H. Sugisawa, T. Baba, $^{207}$Pb chemical shift thermometer at high temperature for magic-angle spinning experiments, Solid State Nucl, Magn. Reson. 15 (1999) 119–123.
[14] M. Concistre, A. Gansmuller, N. McLean, O.G. Johannessen, I.M. Montesinos, P.H.M. Bovee-Geurts, P. Verdegem, J. Lugtenburg, R.C.D. Brown, W.J. DeGrip, M.H. Levitt, Double-quantum $^{13}$C nuclear magnetic resonance of bathorhodopsin, the first photointermediate in mammalian vision, J. Am. Chem. Soc. 130 (2008) 10490–10491.
[15] C.P. Grey, A.K. Cheetham, C.M. Dobson, Temperature-dependent solid-state $^{119}$Sn MAS NMR of $Nd_2Sn_2O_7$, $Sm_2Sn_2O_7$, and $Y_{1.8}Sm_{0.2}Sn_2O_7$. Three sensitive chemical shift thermometers, J. Magn. Reson 101 (1993) 299–306.
[16] B. Langer, I. Schnell, H.W. Spiess, A.-R. Grimmer, Temperature calibration under ultrafast MAS conditions, J. Magn. Reson. 138 (1999) 182–186.
[17] H. Pan, B.C. Gerstein, NMR of $^{31}$P in $(VO)_2P_2O_7$ as an internal temperature standard in high-temperature NMR, J. Magn. Reson. 92 (1991) 618–619.
[18] C.S. Zuo, K.R. Metz, Y. Sun, A.D. Sherry, NMR temperature measurements using a paramagnetic lanthanide complex, J. Magn. Reson. 133 (1998) 53–60.
[19] L.v. Wullen, G. Schwering, E. Naumann, M. Jansen, MAS NMR at very high temperatures, Solid State Nucl. Magn. Reson. 26 (2004) 84–86.
[20] G. Simon, Quartz crystal temperature sensor for MAS NMR, J. Magn. Reson. 128 (1997) 194–198.
[21] R. Tycko, Adiabatic rotational splittings and Berry's phase in nuclear quadrupole resonance, Phys. Rev. Lett. 58 (1987) 2281–2284.
[22] K.R. Thurber, R. Tycko, Biomolecular solid state NMR with magic-angle spinning at 25 K, J. Magn. Reson. 195 (2008) 179–186.
[23] J.S. Frye, G.E. Maciel, Setting the magic angle using a quadrupolar nuclide, J. Magn. Reson. 48 (1982) 125–131.
[24] A. Abragam, Principles of Nuclear Magnetism, Oxford University Press, New York, 2002.
[25] Nuclear spins, moments, and other data related to NMR spectroscopy. in: Lide DR (Ed.) CRC handbook of chemistry and physics. 86 ed. CRC Press, Boca Raton, FL, 2005.
[26] E.G. Wikner, W.E. Blumberg, E.L. Hahn, Nuclear quadrupole spin-lattice relaxation in alkali halides, Phys. Rev. 118 (1960) 631–639.
[27] J.v. Kranendonk, M. Walker, Theory of quadrupolar nuclear spin-lattice relaxation due to anharmonic Raman phonon processes, Phys. Rev. Lett. 18 (1967) 701–703.
[28] J.v. Kranendonk, Theory of quadrupolar nuclear spin-lattice relaxation, Physica 20 (1954) 781–800.
[29] W.T. Berg, J.A. Morrison, The thermal properties of alkali halide crystals. I. The heat capacity of potassium chloride, potassium bromide, potassium iodide and sodium iodide between 2.8 and 270 degrees K, Proc. Royal Soc. London. Ser. A 242 (1957) 467–477.
[30] C.A. Michal, R. Tycko, Stray-field NMR imaging and wavelength dependence of optically pumped nuclear spin polarization in InP, Phys. Rev. B 60 (1999) 8672–8679.
[31] R. Tycko, G. Dabbagh, R.M. Fleming, R.C. Haddon, A.V. Makhija, S.M. Zahurak, Molecular dynamics and the phase transition in solid $C_{60}$, Phys. Rev. Lett. 67 (1991) 1886–1889.
[32] R. Tycko, G. Dabbagh, M.J. Rosseinsky, D.W. Murphy, A.P. Ramirez, R.M. Fleming, Electronic properties of normal and superconducting alkali fullerides probed by $^{13}$C nuclear magnetic resonance, Phys. Rev. Lett. 68 (1992) 1912–1915.
[33] E.R. Andrew, D.P. Tunstall, Spin-lattice relaxation in imperfect cubic crystals and in non-cubic crystals, Proc. Phys. Soc. 78 (1961) 1–11.
[34] T.K. Halstead, P.A. Osment, B.C. Sanctuary, J. Tegenfeldt, I.J. Lowe, Multipole NMR. VII. Bromine NMR quadrupolar echoes in crystalline KBr, J. Magn. Reson. 67 (1986) 267–306.
[35] M. Carravetta, A. Danquigny, S. Mamone, F. Cuda, O.G. Johannessen, I. Heinmaa, K. Panesar, R. Stern, M.C. Grossel, A.J. Horsewill, A. Samoson, M. Murata, Y. Murata, K. Komatsu, M.H. Levitt, Solid state NMR of endohedral hydrogen-fullerene complexes, Phys. Chem. Chem. Phys. 9 (2007) 4879–4894.
[36] T. Maly, G.T. Debelouchina, V.S. Bajaj, K.N. Hu, C.G. Joo, M.L. Mak-Jurkauskas, J.R. Sirigiri, P.C.A. van der Wel, J. Herzfeld, R.J. Temkin, R.G. Griffin, Dynamic nuclear polarization at high magnetic fields, J. Chem. Phys. 128 (2008) 052211.